Molecular Cell, Volume *82*

Supplemental information

Crystal structure of human NADK2 reveals a dimeric organization and active site occlusion by lysine acetylation

Charline Mary, Mona Hoseini Soflaee, Rushendhiran Kesavan, Muriel Gelin, Harrison Brown, G. Zacharias, Thomas P. Mathews, Andrew Lemoff, Corinne Lionne, Gilles Labesse, and Gerta Hoxhaj

Site	Peptide sequence	Peptide modification	Abundance of modification (10^6)	Total peptide abundance (10^6)	% modified peptide	Phosphosite®.
T229	LYLEGtGINPVPVDLHEQQLSLNQHNR	T6(Phospho)	0.08	0.10	80.0	
S289	AsYYEISVDDGPWEK	S2(Phospho)	0.05	70.99	0.07	1 LTP
K76	VVVVAkTTR	K6(Acetyl)	4.85	9.84	49.28	
K98	YAELSEEDLkQLLALK	K10(Acetyl)	0.51	1127.97	0.04	1 HTP
K104	QLLALkGSSYSGLLER	K6(Acetyl)	0.87	5.48	15.87	
K104	QLLALkGSSYSGLLER	K6(Succinyl)	1.62	5.48	29.56	
K170	WADAVIAAGGDGTMLLAASkVLDR	K20(Acetyl)	0.58	516.54	0.11	1 HTP
K176	LkPVIGVNTDPER	K2(Acetyl)	2.11	2585.11	0.08	
K304	QkSSGLNLCTGTGSK	K2(Acetyl)	0.27	0.7	38.57	2 HTP
K317	SSGLNLCTGTGSkAWSFNINR	K13(Acetyl)	ND	459.21	ND	
K339	VATQAVEDVLNIAkR	K14(Acetyl)	4.86	3473.97	0.14	4 HTP
K339	VATQAVEDVLNIAkR	K14(Succinyl)	0.22	3473.97	0.006	1 HTP
K355	ELVEkVTNEYNESLLYSPEEPK	K5(Acetyl)	1.15	5.00	23.00	1 HTP
K397	CFSSkVCVR	K5(Acetyl)	0.71	1.23	57.72	2 HTP

Table S1. Post-translational modifications of NADK2 identified from HEK293E cells expressing NADK2-FLAG. Related to Figure 5. Modified amino acids are shown in red. Percentage of modified peptide represents the ratio of the modified peptide abundance to the total peptide abundance. HTP and LTP refer to high and low throughput data, respectively curated from PhosphoSitePlus®.

Fig. S1

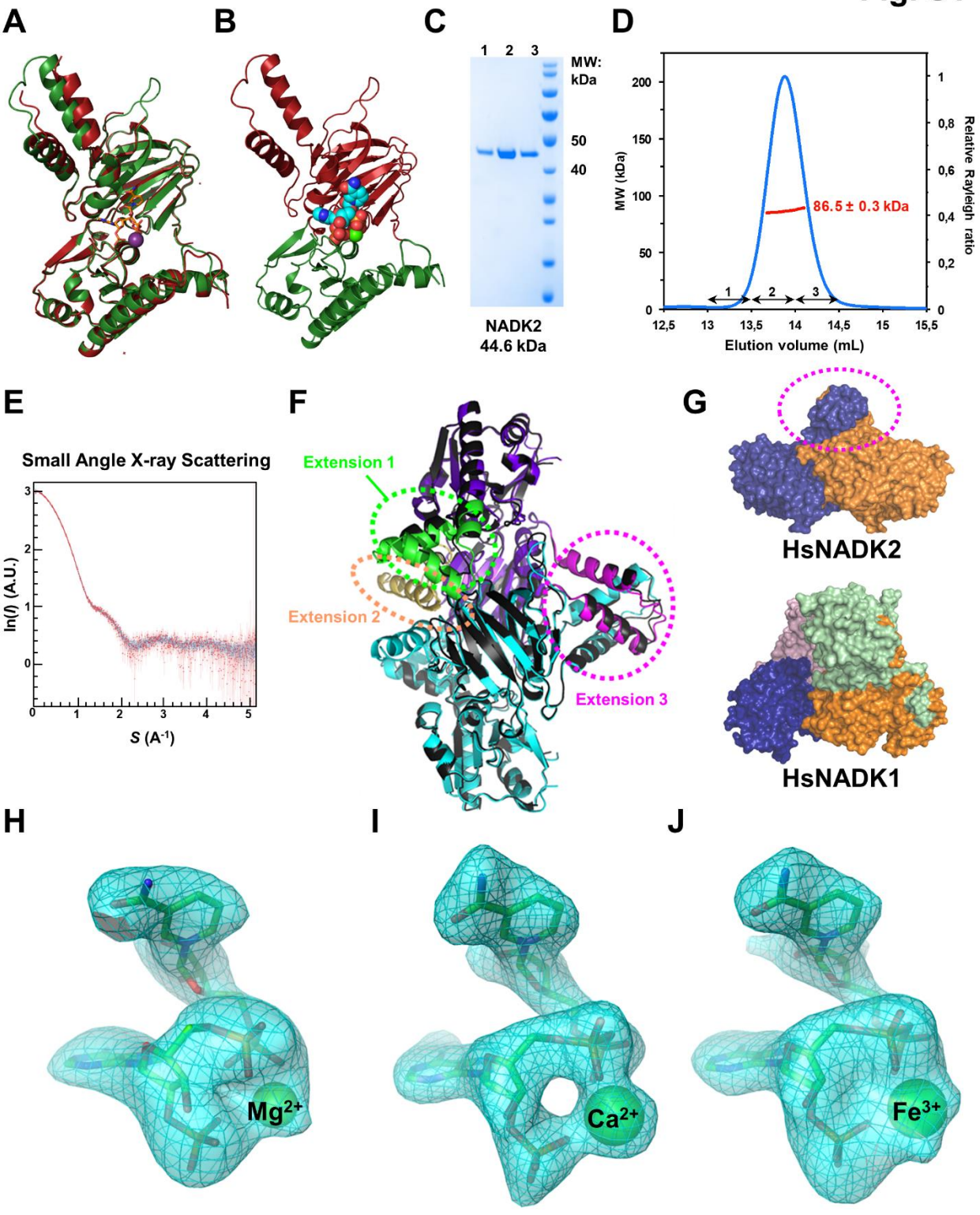
A
B
C
1 2 3
MW: kDa
50
40
NADK2
44.6 kDa
D
MW (kDa)
Relative Rayleigh ratio
86.5 ± 0.3 kDa
Elution volume (mL)
E
Small Angle X-ray Scattering
ln(I) (A.U.)
S (A-1)
F
Extension 1
Extension 2
Extension 3
G
HsNADK2
HsNADK1
H
Mg2+
I
Ca2+
J
Fe3+

Figure S1: Crystal structure of NADK2. Related to Figure 1.

(**A**) Crystal structure of the NADK2 in the apo-form or bound to $NADP^+$. The monomeric structure of NADK2 is shown in red and green ribbons for the NADP-bound and the apo-forms, respectively. The $NADP^+$ molecule (sticks) and the calcium atom (violet sphere) are also shown.

(**B**) Crystal structure of the NADK2 monomer. The monomer crystal structure is colored in green (N-terminal domain) and red (C-terminus domain). The $NADP^+$ molecule (CPK spheres) and the calcium atom (green sphere) are also shown. CPK: Space-filling calotte.

(C) His-NADK2 purity isolated from *E. coli* and subjected to size exclusion chromatography was visualized with Coomassie Blue staining. Lanes 1, 2, 3 indicate the different elution fractions represented on the SEC-MALS elution profile (D).

(D) SEC-MALS elution profile of purified His-NADK2 indicating elution as single peak corresponding to a dimer of 86.5 kDa.

(**E**) SAXS profile of purified NADK2. SAXS experimental data recorded at various concentrations (3, 6, and 12 mg/mL) were scaled to show a similar organization is observed over a large range of concentrations.

(**F**) Comparison of the crystal structure and the AlphaFold model of NADK2. The dimeric crystal structure is shown in a black ribbon. The AlphaFold2 model is colored in cyan for one monomer and in violet ribbon but for the three extensions (shown in green, yellow, and pink ribbons).

(**G**) Comparison of the crystal structures of dimeric NADK2 (top) and cytosolic tetrameric NADK (bottom) (PDB3PFN). The macromolecular surfaces are shown side-by-side for clarity and in the same color code as in Figure. 1B. A dotted pink circle shows extension 3 (aa 325-365), preventing the tetramerization of NADK2.

(H) Electron density around the $NADP^+$ in the NADK2-$NADP^+$-Mg^{2+} complex. The NADP molecule is shown in CPK sticks, and the metal atom is shown as a green sphere. The corresponding electron density was computed as an omit map and the Fourier difference density was contoured at 2.5 σ.

(**I**) Electron density around the $NADP^+$ in the NADK2-$NADP^+$-Ca^{2+} complex. Same as (H), but for the calcium ion shown as a green sphere.

(**J**) Electron density around the $NADP^+$ in the NADK2-$NADP^+$-Fe^{3+} complex. Same as (H), but for the iron ion shown as a green sphere.

Fig. S2

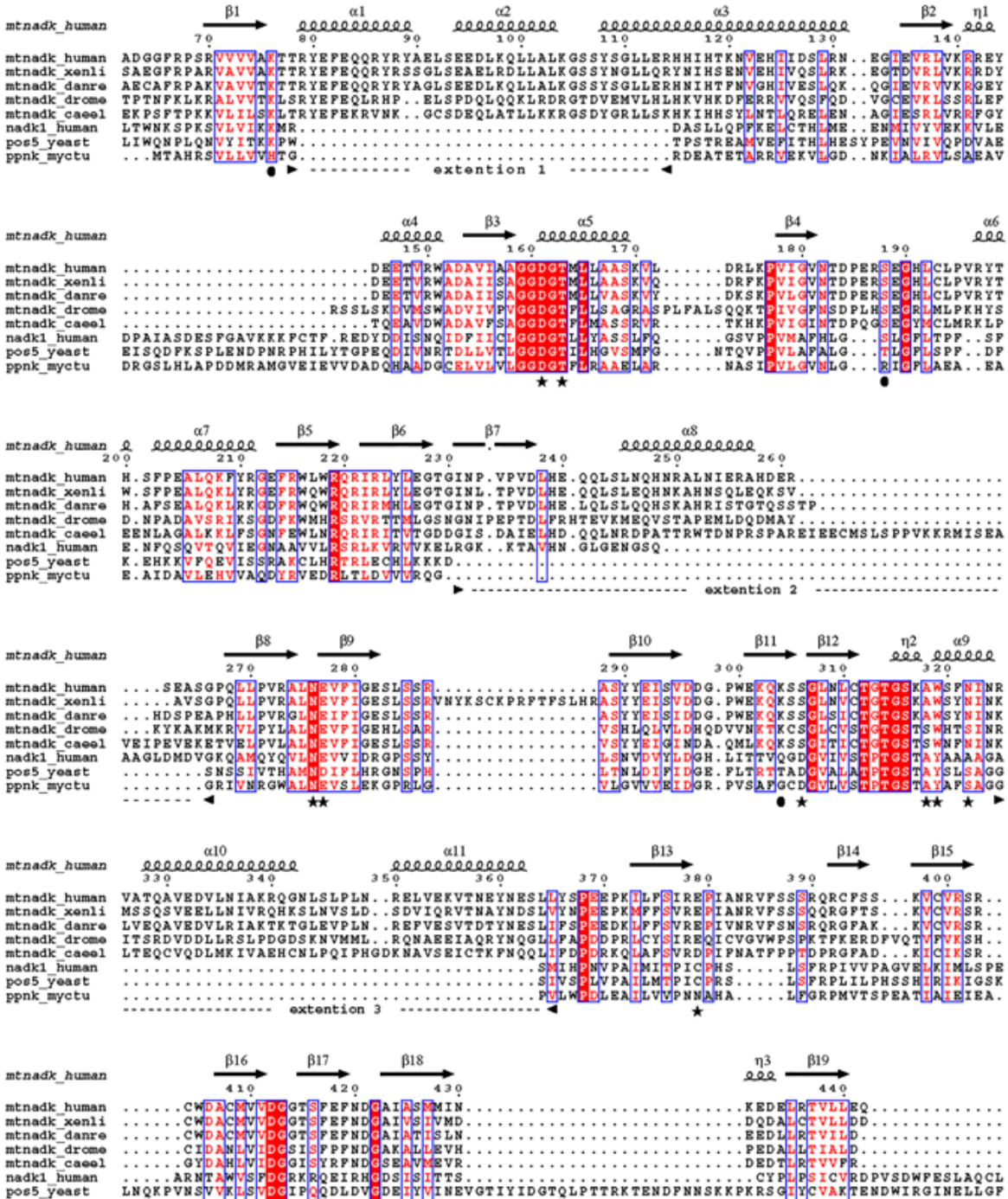
mtnadk_human
mtnadk_human
mtnadk_xenli
mtnadk_danre
mtnadk_drome
mtnadk_caeel
nadk1_human
pos5_yeast
ppnk_myctu
extention 1
extention 2
extention 3

Figure S2. Sequence alignment for NADK2 with several tetrameric NADKs. Related to Figures 1 and 2.

The sequence of the NADK2 from human (Q4G0N4), *D. rerio (Q6DBS0), X. tropicalis* (Q08CZ6*), D. melanogaster* (Q7JW73), *C. elegans* (Q9XXI6) were aligned with the sequence of three tetrameric NADKs (human NADK2 (O95544); yeast mitochondrial NADK (POS5, Q06892) and *M. tuberculosis* NADK *(*ppnK, P9WHV7) using ViTO (Catherinot and Labesse, 2004).

Fig. S3

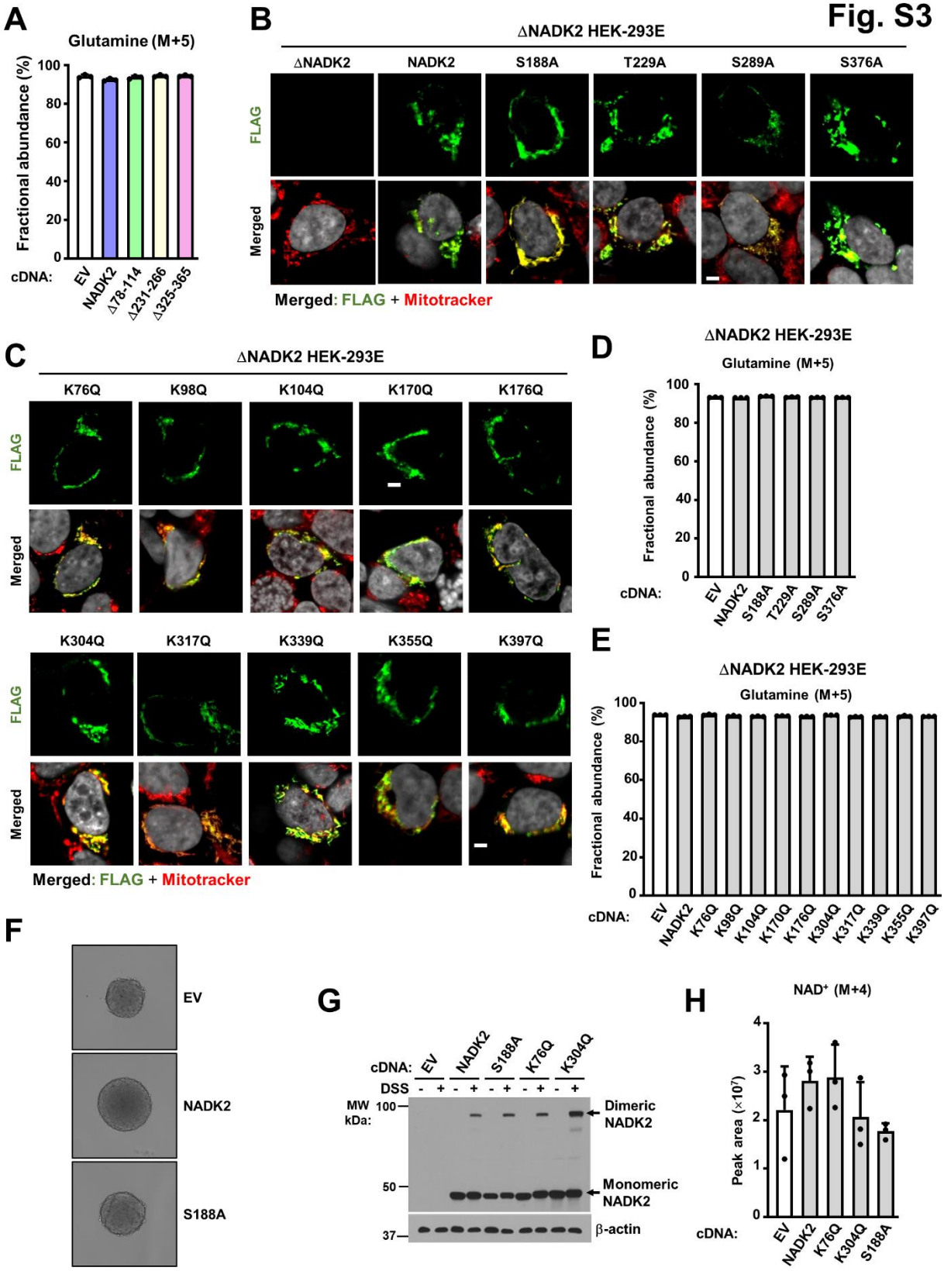
A
Glutamine (M+5)
Fractional abundance (%)
cDNA: EV NADK2 Δ78-114 Δ231-266 Δ325-365
B
ΔNADK2 HEK-293E
ΔNADK2 NADK2 S188A T229A S289A S376A
FLAG
Merged
Merged: FLAG + Mitotracker
C
ΔNADK2 HEK-293E
K76Q K98Q K104Q K170Q K176Q
K304Q K317Q K339Q K355Q K397Q
FLAG
Merged
Merged: FLAG + Mitotracker
D
ΔNADK2 HEK-293E
Glutamine (M+5)
Fractional abundance (%)
cDNA: EV NADK2 S188A T229A S289A S376A
E
ΔNADK2 HEK-293E
Glutamine (M+5)
Fractional abundance (%)
cDNA: EV NADK2 K76Q K98Q K104Q K170Q K176Q K304Q K317Q K339Q K355Q K397Q
F
EV
NADK2
S188A
G
cDNA: EV NADK2 S188A K76Q K304Q
DSS - + - + - + - + - +
MW kDa: 100 50 37
Dimeric NADK2
Monomeric NADK2
β-actin
H
NAD+ (M+4)
Peak area (×10^7)
cDNA: EV NADK2 K76Q K304Q S188A

Figure S3: Mitochondrial localization and function of NADK2 phospho-deficient- and acetylation-deficient mutants. Related to Figures 3 and 5.

(**A**) Fractional abundance of glutamine (M+5) from ΔNADK2 HEK-293E cells stably expressing either empty vector, NADK2 WT, or NADK2 variants with the indicated deleted extensions (Δ78-114, Δ 231-266, Δ 325-365) labeled for 3 h with $^{13}C_5$ glutamine. Related to Fig. 3G.

(**B**) Representative images of localization of the NADK2-Flag WT or S/A variants to mitochondria (red) detected by immunofluorescence with a FLAG epitope antibody (green). ΔNADK2 HEK-293E cells were transiently transfected with NADK2 WT or the indicated NADK2 phospho-mutants (S/A). Mitochondria were stained with MitoTracker™ (red) and nuclei with Hoechst (gray). Scale bars, 2 μm.

(**C**) As in (B), but from NADK2 HEK-293E cells were transiently transfected with NADK2 WT or the indicated NADK2 acetylation-mutants (K/Q). Scale bars, 2 μm.

(**D**) Fractional abundance of glutamine (M+5), but from ΔNADK2 HEK-293E cells stably expressing either empty vector, NADK2 wild-type, or the indicated NADK2 phospho-mutants (S/A) labeled for 3 h with $^{13}C_5$ glutamine. Related to Fig. 5D.

(**E**) Fractional abundance of glutamine (M+5), but from ΔNADK2 HEK-293E cells stably expressing either empty vector, NADK2 wild-type, or the indicated NADK2 acetylation-mutants (K/Q) labeled for 3 h with $^{13}C_5$ glutamine. Related to Fig. 5F.

(**F**) Representative images of spheroids from ΔNADK2 HEK-293E cells stably expressing either NADK2 WT or NADK2 S188A cultured without proline. Related to Fig. 5I.

(**G**) Immunoblots from ΔNADK2 HEK-293E cells transiently transfected with either empty vector (EV), WT NADK2 or NADK2 S188A, K76Q or K304Q that were treated with 1 mM DSS for 1 hour. Monomeric and dimeric NADK2 and the β-actin control are shown.

(**H**) Normalized peak area of mitochondrial NAD^+ (M+4) from labeling with $^{13}C_3$-^{15}N-Nicotinamide (M+4). ΔNADK2 HEK-293E cells stably expressing HA-Mito were transiently transfected with empty vector (EV), WT NADK2 or NADK2 K76Q, K304Q or S188A mutants. Related to Fig. 5L.

Data are presented as the mean ± s.d from n=3 (D, E, H) of biologically independent samples. Data are representative of at least two independent experiments. Multiple comparisons were calculated using one-way ANOVA and Tukey's post hoc test.

Fig. S4

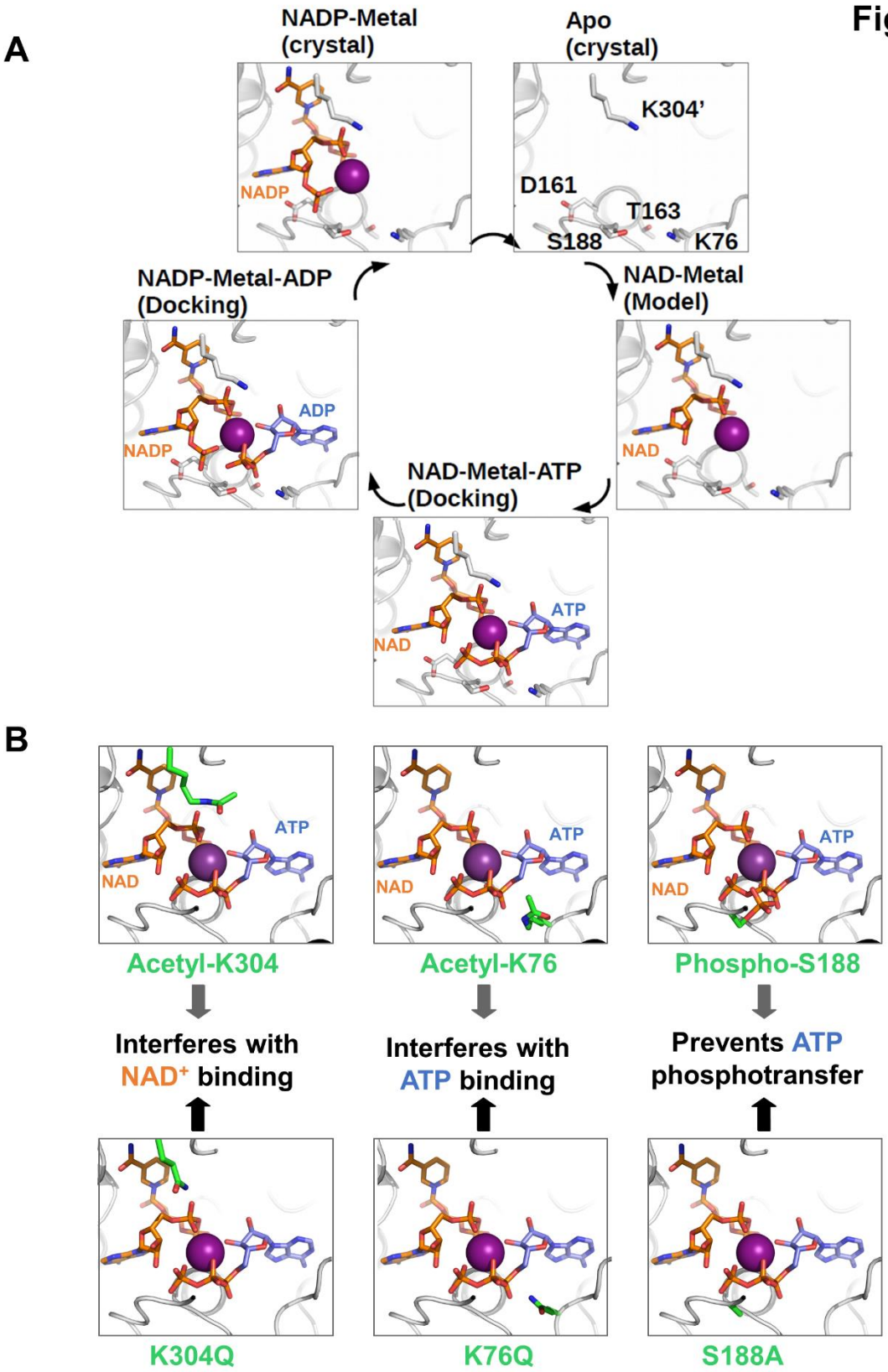
A
NADP-Metal
(crystal)
Apo
(crystal)
K304'
D161
T163
S188
K76
NADP
NADP-Metal-ADP
(Docking)
NAD-Metal
(Model)
ADP
NADP
NAD
NAD-Metal-ATP
(Docking)
ATP
NAD
B
ATP
NAD
ATP
NAD
ATP
NAD
Acetyl-K304
Acetyl-K76
Phospho-S188
Interferes with
NAD+ binding
Interferes with
ATP binding
Prevents ATP
phosphotransfer
K304Q
K76Q
S188A

Figure S4: Structural basis for the regulation of human NADK2 by post-translational modification events. Related to Fig. 5.

(**A**) Enzymatic cycle of NADK2 as deduced from the crystal structures of the $NADP^+$ bound form and the apo form as in Figure 2D, but with the three side-chains neighboring the $NADP^+$ molecule now showing post-translation modification (K76 and S188 from one monomer and K304 from a second monomer). Proteins are in grey ribbon, while ligands are in colored sticks (ATP/ATP are in blue; NAD^+/$NADP^+$ in orange).

(**B**) Schematic representation of the impact of K76 acetylation, K304 acetylation, and S188 phosphorylation (Top panels) or the directed mutagenesis (bottom panels) predicted from manual modeling of the residue modification in the complex with NAD^+ or $NADP^+$, as well as docking of ADP or ATP molecules. Figures were drawn using Pymol. Proteins are in grey ribbon, while ligands are in colored sticks (ATP/ATP are in blue; NAD^+/$NADP^+$ in orange). Mutated or modified side-chains are shown in green sticks.